International Journal of Disaster Risk Reduction 38 (2019) 101228

Contents lists available at ScienceDirect

International Journal of Disaster Risk Reduction

journal homepage: www.elsevier.com/locate/ijdrr

# Community resilience-driven restoration model for interdependent infrastructure networks

Deniz Berfin Karakoc[a], Yasser Almoghathawi[b], Kash Barker[a,*], Andrés D. González[a], Shima Mohebbi[a]

[a] School of Industrial and Systems Engineering, University of Oklahoma, Norman, OK, USA
[b] Systems Engineering Department, King Fahd University of Petroleum and Minerals, Dhahran, Saudi Arabia

ARTICLE INFO

*Keywords:*
Interdependent networks
Community resilience
Restoration
Optimization

ABSTRACT

Critical interdependent infrastructure networks such as water distribution, natural gas pipeline, electricity power, communication and transportation systems provide the essential necessities for societies and their utilization is the backbone of everyday processes such as production, health, convenience and many more. Often cascading dysfunctionality or disruption in these critical infrastructure networks triggers chain reactions of blackouts or blockages through the system of highly interconnected infrastructure networks, and the disruption of surrounding societies. For the planning of restoration processes and resilience of these, social aspects and demographics should also be considered to assign and mitigate the possible social risks associated with these disruptions. In this work, we study the restoration planning of critical interdependent infrastructure networks after a possible disruptive event by mainly emphasizing on the vulnerability indices of interacting society. We integrate (i) a resilience-driven multi-objective mixed-integer programming formulation to schedule the restoration process of disrupted network components in each network with (ii) an index of social vulnerability that is geographically distributed. We present an illustrative example of the proposed integrated model that focuses on studying the community resilience in Shelby County, TN, United States.

## 1. Introduction

Modern societies heavily rely on the sustainability and proper performance of critical infrastructure networks. Two decades ago, the Report of the President's Commission on Critical Infrastructure Protection [1] defined a critical infrastructure network as a "network of independent, mostly privately-owned, man-made systems and processes that function collaboratively and synergistically to produce and distribute a continuous flow of essential goods and services." These critical infrastructure networks, such as water distribution, electric power, natural gas, communication, and transportation systems, are essential for providing the basic human needs of society and maintaining its quality of life. More recently, the Infrastructure Security Partnership [2] emphasized the importance of forming physically interdependent infrastructure networks that are resilient against the disruptions that will eventually occur. It defined resilient infrastructure networks as the networks that should "prepare for, prevent, protect against, respond or mitigate any anticipated or unexpected significant threat or event" and that are able to "rapidly recover and reconstitute critical assets, operations, and services with minimum damage and disruption." There exists a need for resilience-driven planning to maintain "secure, functioning, and resilient critical infrastructures" [3]. The National Infrastructure Protection Plan [4] notes the risk imposed by the interdependencies among these networks and the importance of addressing these issues as it is "essential to enhancing critical infrastructure security and resilience" against inevitable disruptions due to natural disasters, malevolent attacks, and age-driven failures.

While measuring the vulnerability of infrastructure networks by either topological descriptors [5–8] or by flow-based descriptors [9–12] has been a well-studied problem, the restoration of infrastructure networks has been an important area of study for the last decade, particularly from an optimization perspective. The stochastic integer program proposed by Xu et al. [13] determines the schedule of inspection, damage assessment, and repair tasks that optimize the power network restoration. Yan and Shih [14] proposed a multi-objective, mixed-integer programming method with the objective of minimizing the total time of repair and relief distribution after a disruption in a transportation network. Similarly, Matisziw et al. [15] developed a multi-objective optimization model to maximize the total system flow while minimizing the system cost through the recovery of a communication

* Corresponding author. School of Industrial and Systems Engineering, University of Oklahoma, 202 W. Boyd St., Rm. 124, Norman, OK, 73019, USA.
*E-mail address:* kashbarker@ou.edu (K. Barker).

https://doi.org/10.1016/j.ijdrr.2019.101228
Received 18 February 2019; Received in revised form 28 June 2019; Accepted 30 June 2019
Available online 03 July 2019
2212-4209/ 

system. The integer programming model by Nurre et al. [16] considers the maximization of the cumulative weighted flow in the infrastructure networks by scheduling work crews to restore disrupted components. Aksu and Ozdamar [17] proposed a dynamic path based mathematical model to maximize network accessibility by scheduling debris removal. Vugrin et al. [18] developed a bi-level optimization model for network recovery, providing the recovery sequence that maximizes the total flow in a critical infrastructure network. The multi-objective optimization model developed by Kamamura et al. [19] focuses on the recovery of transportation systems by maximizing the traffic recovery ratio and minimizing the number of switched transportation paths in each stage of a multi-stage restoration process. Finally, Fang et al. [20] proposed a Monte Carlo simulation-based method to rank the disrupted components according to their impact on system resilience to order their recovery. In general, the previously proposed algorithms commonly cover the objective of maximizing the performance of infrastructure networks, rebuilding the disrupted components and their functionality by assigning those components to work crews, and determining the order of restoration sequence in the aftermath of a disruption. However, notably absent in these studies is the perspective of the communities that rely on infrastructure networks and that are adversely impact during their disruption. Hence, in this study we model the restoration scheduling of critical interdependent infrastructure networks from a community resilience perspective.

As noted by Rinaldi et al. [21]; physical infrastructure networks do not exist and function on their own in an isolated environment. In fact, they often rely heavily on each other in various ways. The interdependency of infrastructure networks has been categorized into four groups [21]: (i) physical, where output from one infrastructure network serves as an input to another, (ii) cyber, where one network depends on the information transmitted from another, (iii) geographical, where two infrastructure networks can be affected by the same local disruptive event, and (iv) logical, for all other possible types of dependency. In this study, we focus on the *physical* interdependency among three major infrastructure networks, though the proposed approach is generalizable for considering other types of interdependencies as well.

Interdependencies among infrastructure networks become more frequent and complex due to the increasing trend of globalization and technological developments [21–24, 84]. Even though the interdependencies can improve the efficiency of network functionality, this type of complex coordination cause them to become more vulnerable to disruptions. As a result of the interdependency, a disruption in some components of one of the infrastructure networks could lead a dysfunctionality in the undisrupted components of other dependent networks and could result in a series of cascading failures among the whole infrastructure network system [25–28]. Therefore, this high vulnerability of infrastructure networks against disruptions is a critical concern for decision makers where they should account for the interdependencies through the recovery planning to achieve a realistic performance analysis [29]. Moreover, scheduling the restoration processes separately for interdependent infrastructure networks without considering their interdependencies could cause misutilization of resources, waste of time and funds, and even might trigger additional inoperability of distribution systems [30]. However, functional connectivity among these critical infrastructures is not the only dependency that should be taken into account. The supply-demand relationship, thus an existence-based dependency that exists within infrastructure networks, is another challenging aspect that should be addressed in restoration scheduling models.

As infrastructure networks exist to enable the fundamental services that support the economic productivity, security, and quality of life of the community, interdependency among infrastructures is not the sole interdependency of interest in this study. The relationship among infrastructure and community networks, defined as the interconnected society that infrastructure networks support [31], is generally depicted in Fig. 1. Among the planning documents by government agencies on resilience, there is a particular emphasis on the resilience of communities after a disruptive event. The National Academies of Science [32] suggests "One way to reduce the impacts of disasters on the nation and its communities is to invest in enhancing resilience […]." Some of the many various explanations of the concept of community resilience in the literature can be summarized by the National Institute for Standards and Technology [85], which defines community resilience as "the ability of a community to prepare for anticipated hazards, adapt to changing conditions, and withstand and recover rapidly from disruptions." Additionally, according to Rotmans et al. [33] and Resilience Alliance [34]; community resilience is the ability of a community to successfully cope with disruptions from the economic, social, and environmental aspects, as well as to coordinate recovery activities. From a more social sciences-based perspective, the relationship between physical systems and social communities has been recognized for several years. The 1994 World Conference on Natural Disaster Reduction emphasized building disaster risk reduction frameworks that specifically address the impacts of the social norms [35]. Assessing the human occupancy in hazard zones and understanding the human dimensions of disasters was a feature of disaster risk reduction studies [36,37], where various scientific assessments for developing disaster-resistant communities are introduced in the literature [38,39]. Furthermore, research for defining disaster resilience in terms of the adaptive capacities of individuals [40,41], communities [42,43], and larger societies [44,45] have gained prominence [46,47]. The Subcommittee on Disaster Risk Reduction [48] states that "… with consistent factors and regularly updated metrics, communities will be able to maintain report cards that accurately assess the community's level of disaster resilience. This, in turn, will support comparability among communities and provide a context for action to further reduce vulnerability," where it is assumed that assessing and enhancing the community resilience is one of the grand challenges in planning disaster reduction strategies. Therefore, based on the general understanding of the community resilience concept from both engineering and social sciences perspectives, communities contribute to the overall impact of a disruption and should be considered in restoration and resilience enhancement processes.

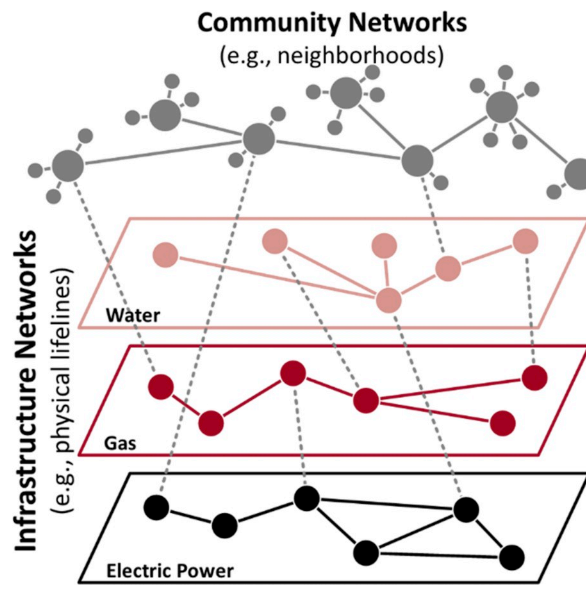

**Fig. 1.** Relationship between physical infrastructure and community networks (adapted from Barker et al. [31]).

In this paper, we study the restoration of interdependent infrastructure networks from the perspective of community impact, as measured by socio-economic and demographic information describing the affected communities. We make use of social vulnerability indices [49] and population densities of the service areas to represent community impact, thus guiding the restoration process toward areas of potential community need. The primary objective of this study is to: (i) integrate a resilience-driven multi-objective mixed-integer programming formulation to schedule the restoration of disrupted components in each network, (ii) assign the restoration of these components to specific work crews, and (iii) prioritize them with social vulnerability indices and densities of the serviced population to account for the impacts on the geographically surrounding community.

## 2. Background

In this section, we address the relevant methodological background on network resilience measures, independent infrastructure network recovery problems, and social vulnerability indices.

### 2.1. Modeling and measuring network resilience

The general terminology of resilience is often considered to be the ability to withstand, adapt to, and recover from a disruption [3]. While many generally agree on the definition that is introduced by Obama [3] (e.g., Haimes [50]; Aven [51] and Ayyub [52]), a number of different approaches to measure and model system resilience have been proposed in the recent literature [53]. For example, Cimellaro et al. [54] measured the resilience of a system as the normalized area underneath a function describing the performance of the system, while Rosenkrantz et al. [55] represented system resilience as a function of topological measures, and Li and Lence [56] quantified system resilience as the probability of failure recovery, among others.

However, in this study, we quantify the resilience of a system of networks by adopting the paradigm proposed by Henry and Ramirez-Marquez [57]. Denoted as Я, the resilience of a network at time $t$ is formulated as $Я(t|e^j) = \text{Recovery}(t)/\text{Loss}(t_d)$, for disruptive event $e^j$ and where $t_d < t < t_f$ as shown in Fig. 2. The two primary dimensions of network resilience are *vulnerability* and *recoverability* [57,58]. Jönsson et al. [59] defined the vulnerability of a network as "the magnitude of damage in network performance due to a disruptive event" and recoverability could be described as "the speed at which the network reaches to a desired performance level" [60]. Through our proposed approach, among all the above introduced explanations in the literature, we adopted the system resilience measure proposed by Henry and Ramirez-Marquez [57].

### 2.2. Restoring interdependent infrastructure networks

Attention has recently been devoted to studying the optimal scheduling of restoration resources for interdependent infrastructure networks. Lee et al. [61] proposed an interdependent layered network model using mixed-integer programming with the objective of minimizing the sum of costs associated with flow and slack through time, where cost and available work crews for restoration were not accounted for. Gong et al. [62] proposed an optimization model for the restoration of disrupted interdependent network components assuming that the predetermined due dates of these components as the upper-limit on the completion of the restoration process are known through the study. Their multi-objective restoration scheduling model was solved using Benders decomposition with the objective of minimizing the cost, tardiness, and makespan. Coffrin et al. [63] proposed an integrated mixed-integer programming method to maximize the weighted sum of interdependent met demand through the recovery duration. Cavdaroglu et al. [64] and Sharkey et al. [65] proposed mixed-integer programming models to determine the set of disrupted components that should be restored and to assign them to available work crews with the objective of minimizing the sum of flow cost, slack cost, and the cost associated with the restoration process (e.g., installation and assignment of disrupted components). Holden et al. [29] studied an extended network-flow model at a local-scale of physically interdependent infrastructure networks to simulate their performance by providing a linear programming optimization model that minimized the total cost of production, commodity flow, storage, discharge, and slack demand. González et al. [66] proposed the Interdependent Network Design Problem (INDP), which focuses on finding the optimal recovery strategy of a system of interdependent networks, while considering limited resources, possible savings due simultaneous repairs of co-located components, and other budget and operational constraints. Smith et al. [67] proposed a game-theory-based model to study and optimize the recovery of system of interdependent networks when each network is separately managed by a different entity (or player). González et al. [68] proposed a data-driven system identification approach that uses a linear operator (defined as the recovery operator) to depict the main damage and recovery dynamics of a system of interdependent networks, which later on can be used to efficiently generate quasi-optimal recovery strategies. Baidya and Sun [30] formulated a mixed-integer linear programming approach to prioritize the restoration activities of disrupted components in the physically interdependent power and communications infrastructure networks with the objective of minimizing the number of energizing activities required through the restoration to ensure the operability of every node. Tootaghaj et al. [69] proposed a two-phase recovery approach for physically interdependent power and communications network while assuming that the disruption occurred only in the power network. First, the formulation of a linear programming model for minimum flow cost assignment problem to avoid further failures in the system is completed. The objective of this

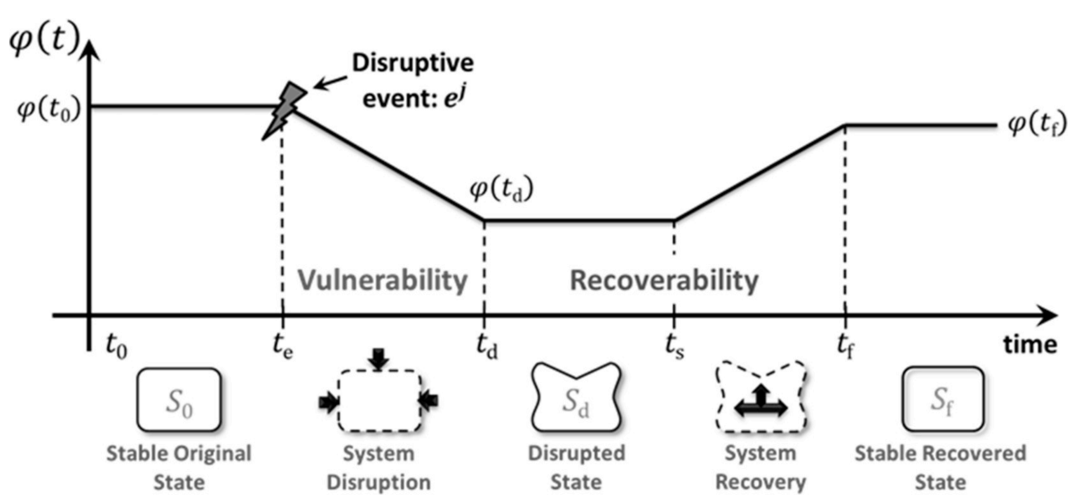


**Fig. 2.** Network performance representation $\varphi(t)$, across various stages of a disruptive event (adapted from Henry and Ramirez-Marquez et al. [57]).

model is finding the setting of the power flow which avoids further cascading. Then, the formulation of a mixed-integer programming for the recovery problem of these interdependent infrastructure networks in order to provide the schedule of recovery for the disrupted components took place. The objective of this approach is to maximize the total amount of commodity delivered through both networks (i.e. electricity power) in the recovery duration. Zhang et al. [70] proposed an optimization model to determine the allocation of available restoration resources (i.e., time and work crews) and the optimal budget associated with the restoration process after a specific disruption scenario for the physically interdependent infrastructure networks while the resilience of the system is enhanced. In the literature, even though the restoration scheduling of interdependent infrastructure networks has been examined both with network performance and a resilience perspective in mind, accounting for the resilience of communities is the most important contribution of this work.

In this study, we propose a general approach to account for community resilience in a multi-objective optimization model (adopted from Almoghathawi et al. [71]). The model considers time availability and specific skill requirements in the work crews for the restoration of disrupted components (i.e., each network has been assigned with separate work crews for the restoration process, differentiated based on their ability restore a distinct type of infrastructure). The two objectives of our proposed model are developed based on the two major concerns of potential decision makers for an infrastructure network restoration problem which are (i) enhancing system resilience and ensuring a desired level of operability in a timely manner, and (ii) achieving this goal under a certain budget expectation. Therefore, the two objectives of our proposed model are (i) maximizing the resilience of studied interdependent infrastructure networks, and (ii) minimizing the costs associated with the disruption, resulting unsatisfied demand, and restoration. Discussed subsequently and suggested as one of the major improvement for the already existing interdependent infrastructure network restoration problem, the model proposed in this paper additionally accounts for the social vulnerability and population densities associated with the disrupted components of the interdependent networks. Through the restoration planning process, our approach prioritizes the restoration of disrupted components that serve to socially more vulnerable and denser areas in the complete study region. Therefore, our model integrates a community resilience perspective by reformulating system resilience. Hence, relative to the existing literature, our approach mainly considers the well-being of the served community and emphasizes a broader humanitarian motivation for interdependent infrastructure network restoration problem.

### 2.3. Characterizing social vulnerability

Various aspects have been studied for measuring the vulnerabilities of the systems that are caused by their surrounding environment. Mileti [38] stated that the external vulnerabilities that would impact the overall system fragility could be formed by three major elements due to its interaction with them. These three aspects are defined as (i) the surrounding physical environment, (ii) the social and demographic characteristics of the related community, and (iii) the built structures that are included in the system. Thus, Mileti [38] utilized spatially-explicit information such as the location of nodes and links in the network and their capacities in as-planned operating conditions to characterize vulnerabilities. Additionally, to assign the indicators of vulnerability of the built environment, different approaches have been introduced such as the evacuation potential (in arterial miles/mi$^2$) of the studied area [72] and the housing age (% of houses that are built between 1970 and 1994) in that location, among others. Moreover, many studies have been conducted to characterize service networks and their vulnerabilities. These studies generally focus on quantifying the vulnerabilities that are shaped by the ability or inability of the related region to mitigate risk. Thus, these studies mostly accounted for vulnerabilities by identifying the number of work crews in the area, amounts of available resources (i.e., restoration equipment), their dispatch locations, numbers of physicians in the region [47], shelter capacity [73], and the medical capacity of the disrupted location [74]. To address the baseline conditions for community networks, the proposed algorithms described the existing vulnerabilities generally by accounting for spatially explicit populations and work locations, but also by considering static indicators of resilient communities. These static indicators mostly capture societal characteristics such as racial/ethnic inequality [36,47], educational inequality [47,75], previous disaster experience [36], and the social vulnerability index (SoVI) [49,73,75]. Among these approaches to address the vulnerabilities that arise due to the surrounding social environment, SoVI-based methods provide a comprehensive perspective of socio-economic attributes.

Social vulnerability is defined as the set of characteristics of an individual or a group that influence their capacity to anticipate, cope with, resist and recover from the impact of a hazard [76]. Hence, social vulnerability is often measured as a function of the socio-economic conditions of the communities that represent their inherent vulnerabilities that influence their ability to respond to a disruptive event. Thus, even if different communities are exposed to similar disruptive events, the associated consequences will differ due to their diverse socio-economic conditions. The SoVI algorithm is a popular means to quantify these conditions [49]. Through this algorithm, the inherent vulnerabilities in society are quantified by the differences between the percentages of each socio-economic sub-group. These sub-groups generally represent the members of the society that, according to Cutter et al. [49]; are more fragile and more dependent on the support of external resources in times of crisis. To measure social vulnerability, Cutter et al. [49] identified 42 variables that represent different socio-economic properties and the existing levels of these properties through society. With these 42 variables all the existing demographic categories to define a community are covered, whereas these variables are clustered into 11 related groups. These 11 factor groups are categorized mostly around age, gender, race, wealth, and occupation of the members of the community, as listed in Table 1.

According to the definitions and percentages of these factors, these various properties either contribute to or degrade the social vulnerability of a region. By utilizing these 11 factor groups, Cutter et al. [49] then developed a social vulnerability index algorithm to calculate the vulnerability of spatially explicit communities, suggesting that the utilization of available resources through the pre- and post-disruption stages may differ for each community.

In our study, a reduced version of the SoVI algorithm, SoVI-Lite [77,78], is utilized to measure the potential of community loss and possible community response after a disruption. Thus, the SoVI-Lite algorithm is used here to guide the restoration scheduling problem, thus adding a community resilience perspective to physical infrastructure network restoration.

The SoVI-Lite algorithm calculates the social vulnerability index for a given community with the following three steps: (i) obtaining the percentage of the population in that community that belongs to the social group categorized by the 42 variables to define socio-economic vulnerabilities, then (ii) calculating the $z$-scores for each of the 42 variables by using the overall mean and standard deviation per factor,

**Table 1**
The 11 factor groups that are identified by Cutter et al. [49] to quantify the social vulnerability of a community.

| | |
|---|---|
| Age | Occupation |
| Density of the built environment | Personal wealth |
| Ethnicity (Hispanic) | Race (African-American) |
| Ethnicity (Native American) | Race (Asian) |
| Housing stock and tenancy | Single-sector economic dependence |
| Infrastructure dependence | |

and finally (iii) taking the sum of $z$-scores of all 42 variables to account the total social vulnerability index of a specific region. Furthermore, the social vulnerability indices are standardized to be scaled between 0 and 1 as in Eq. (1) where 1 represents socially the most vulnerable community and 0 stands for socially the most resilient community. By standardizing, any negative social vulnerability scores would be avoided without changing the probability distribution, and the scores can be integrated in the proposed optimization model without conflicting with the resilience metric and total recovery cost formulation.

$$\frac{z-\min(X)}{\max(X)-\min(X)}, \quad \forall\, z \in X \tag{1}$$

## 3. Proposed methodology

We reformulate an initial multi-objective resilience-driven restoration optimization model proposed by Almoghathawi et al. [71]. This adopted mixed-integer program maximizes the resilience of the interdependent infrastructure networks while minimizing the total cost associated with the restoration process. The major contribution of this work is the introduction of social vulnerability and population density measures to account for a community resilience perspective on infrastructure network restoration.

### 3.1. Notation and assumptions

The following assumptions have been made in the development of the restoration model (i) the components of all infrastructure networks (i.e., nodes and links): are either undisrupted or fully disrupted, (ii) the recovery durations can vary for each component in each network, (iii) disrupted components cannot be operational until they have been fully recovered, (iv) a known demand, supply, and flow capacity are assigned to each demand node, supply node, and link, respectively, for each network, (v) known and fixed costs associated with unmet demand (i.e., disruption cost) are assigned to demand nodes and varying restoration costs are assigned to disrupted nodes in each network, (vi) known and varying unit flow costs and restoration costs are assigned to each link in each infrastructure network, (vii) physical interdependency is defined such that a component can operate fully (or cannot operate at all) if the component it depends on from either the same or different network is fully operating (or not operating at all), (viii) a known and fixed number of available work crews for the restoration process is assigned to each network, and finally (ix) the assigned work crews can restore a single disrupted component in each infrastructure at a time. Most of these constraints that govern the component functionality, recoverability, disruption, and interdependency can be loosened (e.g., Morshedlou et al. [79]) so that they are represented by continuous rather than binary states.

Set $K$ represents the set of infrastructure networks, and $T=\{1,\dots,\tau\}$ represents the set of available time periods for the restoration process. For each network $k \in K$, the sets of nodes and links are represented by $N^k$ and $L^k$, respectively, where set of supply nodes and set of demand nodes are denoted by $N_s^k \subseteq N^k$ and $N_d^k \subseteq N^k$ respectively. The set of disrupted nodes are denoted by $N'^k$ and the set of disrupted links are represented by $L'^k$. The maximum amount of supply at node $i \in N_s^k$ in network $k \in K$ is denoted by $b_i^k$, calculated as the maximum flow from node $i \in N_s^k$ to all demand nodes $i \in N_d^k$ in network $k \in K$. The amount of unmet demand at node $i \in N_d^k$ in network $k \in K$ at time $t \in T$ is represented with $s_{it}^k$. Thus, the total unsatisfied demand at all demand nodes in network $k \in K$ through the restoration process at time $t \in T$ is $\sum_{i \in N_d^k} s_{it}^k$. The unmet demand at demand node $i \in N_d^k$ in network $k \in K$ after the disruptive event is denoted by $Q_i^k$, and the equal weight of each network is represented by $\mu^k$ for network $k \in K$, such that $\sum_{k \in K} \mu^k = 1$.

The cost of restoration of disrupted nodes and links in network $k \in K$ are represented as $fn_i^k$ for $i \in N'^k$ and $fl_{ij}^k$ for $(i,j) \in L'^k$, respectively. The unitary unsatisfied demand cost associated with node $i \in N_d^k$ is represented with $p_i^k$, while the unitary flow cost through link $(i,j) \in L^k$ is represented with $c_{ij}^k$. The binary variable $z_i^k$ is equal to 1 if node $i \in N'^k$ is restored and 0 otherwise. Likewise, binary variable $y_{ij}^k$ is equal to 1 if link $(i,j) \in L'^k$ is restored and 0 otherwise. The total flow through link $(i,j) \in L^k$ in network $k \in K$ and at time $t \in T$ is represented by non-negative variable $x_{ijt}^k$.

The restoration duration for node $i \in N'^k$ and for link $(i,j) \in L'^k$ are denoted by $dn_i^k$ and $dl_{ij}^k$ that are proportional to the capacity of the nodes and length of the links in the networks, respectively. The flow capacity for link $(i,j) \in L^k$ in network $k \in K$ is $u_{ij}^k$. The binary variable $\beta_{it}^k$ is equal to 1 if the node $i \in N^k$ is operational and 0 otherwise, and the binary variable $\alpha_{ijt}^k$ is equal to 1 if the link $(i,j) \in L'^k$ is operational and 0 otherwise in network $k \in K$ at time $t \in T$. The set of available work crews or resources for the restoration process of each network $k \in K$ is represented with $R^k$, where the resources are assigned specifically for each network in terms of the required skills and expertise. $\gamma_{it}^{kr}$ and $\delta_{ijt}^{kr}$ represent the scheduling variables for node $i \in N'^k$ and link $(i,j) \in L'^k$ in network $k \in K$ and at time $t \in T$, respectively. These variables are both equal to 1 if the restoration of the associated disrupted component is completed by work crew $r \in R^k$ at time $t \in T$ and 0 otherwise. Finally, the network interdependencies are represented by $((i,k),(\bar{i},\bar{k})) \in \Psi$, where node $\bar{i} \in N^{\bar{k}}$ in network $\bar{k} \in K$ is physically dependent to node $i \in N^k$ in network $k \in K$ in terms of functionality.

### 3.2. Community resilience measures

We introduce the social vulnerability index by defining a parameter $SoVI_i^k$, which represents an index between 0 (socially the least vulnerable) and 1 (socially the most vulnerable) for demand node $i \in N_d^k$ in network $k \in K$. The value of $SoVI_i^k$ is calculated by the SoVI-Lite method separately for each demand node according to the geographical region the node covers. Moreover, to give relatively more emphasis on the regional areas that are assigned with higher social vulnerability indices (i.e., 0.7 and higher values of $SoVI_i^k$), we introduce the exponential formulation of social vulnerability scores, which is represented as $V_i^k$, as in Eq. (2). Hence, with this formulation we highly penalize the increases in the social vulnerability scores for more vulnerable areas, as it is difficult to discern the relative importance of SoVI values alone. The constant $a$ in Eq, (2) is chosen such that it would generate a reasonable emphasis on higher social vulnerability scores without causing computational delays.

$$V_i^k = e^{a \times SoVI_i^k}, \quad \forall\, i \in N_d^k,\, a \in Z^+ \tag{2}$$

To account for human occupancy levels in our resilience-driven objective, we introduce the parameter $P_i^k$ to indicate the population density of the geographical region in which the demand node is located. The population density measure is based on the addresses of the residents in the study area and does not reflect dynamic population changes throughout the day. In addition to SoVI-driven measures of social vulnerability, the size of the population being served by infrastructure demand nodes can also be considered as a perspective of community resilience. The formulation to represent the population density served by demand node $i \in N_d^k$ is shown in Eq. (3).

$$P_i^k = \frac{\text{population of the service area served by demand node } i}{\text{total population of all service areas}}, \quad \forall\, i \in N_d^k \tag{3}$$

### 3.3. Optimization model

The complete version of the proposed optimization model with the focus of two objective functions to (i) maximize the resilience for a set of interdependent infrastructure networks and (ii) minimize the total cost associated with the restoration process is as follows. These two conflicting objectives and the constraints defined through the development of our model are explained in a more detailed way in this section.

We measure resilience as a function of unmet demand $s_{it}^k$, for demand node $i \in N_d^k$ in network $k \in K$ through recovery time $t \in T$, where increase in the slack demand represents the loss in the maximum flow due to a disruption as seen in Eq. (4). The loss in demand at demand node $i \in N_d^k$ in network $k \in K$ right after the disruption is denoted by $Q_i^k$, and $\sum_{i\in N_d^k} Q_i^k$ measures the total unmet demand in network $k \in K$ before the recovery activities commence. In this case, $\sum_{i\in N_d^k} Q_i^k$ represents the maximum amount of unmet demand in the infrastructure network, and it is assumed network performance cannot exceed its original value after recovery. Further, we introduce the importance of demand nodes from a community resilience perspective with parameters $V_i^k$ and $P_i^k$ for demand node $i \in N_d^k$ in network $k \in K$, representing social vulnerability and population density, respectively. In the resilience objective function $\sum_{k\in K}\left(\sum_{i\in N_d^k}(Q_i^k V_i^k P_i^k) - \sum_{i\in N_d^k}(s_{it}^k V_i^k P_i^k)\right)$ denotes the amount of slack restored at each recovery period $t \in T$. Since reducing the total amount of unmet demand means increasing the flow that has been carried through the interdependent infrastructure network, it states increasing the performance of the interdependent networks. Hence, improving the effectiveness of the infrastructure network and its ability to recover the maximum amount of possible slack through the recovery, given the prioritization of the demand nodes according to the social vulnerability scores and population densities of the region they represent, is denoted in the resilience objective as in Eq. (4).

$$\max \sum_{k\in K} \mu^k \sum_{t=1}^{\tau} \left( \frac{\sum_{i\in N_d^k}(Q_i^k V_i^k P_i^k) - \sum_{i\in N_d^k}(s_{it}^k V_i^k P_i^k)}{\sum_{i\in N_d^k}(\tau Q_i^k V_i^k P_i^k)} \right) \tag{4}$$

For the cost objective in Eq. (5), we consider three different cost categories that are associated with the restoration process of the system. The flow cost, $c_{ij}^k$, represents the unitary cost of carrying flow through link $(i, j) \in L^k$ in network $k \in K$ in the system. The varying restoration costs, $fn_i^k$ for node $i \in N'^k$ and $fl_{ij}^k$ for link $(i, j) \in L'^k$ denotes the cost associated with the available resources and their utilization in the restoration process of disrupted components where these costs are proportional to the supply capacity of the nodes and the length of the links in the networks. Finally, the disruption cost $p_i^k$ for node $i \in N_d^k$ quantifies the penalty cost for unmet demand due to the disruptive event. Additionally, we assign social vulnerability scores and population densities to penalty costs for disrupted demand nodes. In the objective, $\sum_{k\in K}\sum_{i\in N_d^k}(p_i^k s_{it}^k V_i^k P_i^k)$ assumes that delaying or postponing the recovery of socially more vulnerable and denser areas should be penalized more heavily than the socially less vulnerable and less dense areas since socially more vulnerable sub-groups would suffer more if the resource investments (i.e., time and work crews) for the restoration of these areas are not prioritized [49]. Hence, minimizing the cost objective of our model also considers the recovery of all demand nodes that are associated with highly vulnerable and more populated regions to support the community resilience perspective.

$$\min \sum_{k\in K}\left( \sum_{i\in N'^k} fn_i^k z_i^k + \sum_{(i,j)\in L'^k} fl_{ij}^k y_{ij}^k + \sum_{t\in T}\left[ \sum_{(i,j)\in L^k} c_{ij}^k x_{ij}^k + \sum_{i\in N_d^k} p_i^k s_{it}^k V_i^k P_i^k \right]\right) \tag{5}$$

The two objectives above are balanced for the following constraints.

$$\sum_{(i,j)\in L^k} x_{ijt}^k \le b_i^k, \quad \forall\, i \in N_s^k,\, k \in K,\, t \in T \tag{6}$$

$$\sum_{(i,j)\in L^k} x_{ijt}^k - \sum_{(j,i)\in L^k} x_{jit}^k = 0, \quad \forall\, i \in N^k \backslash \{N_s^k, N_d^k\},\, k \in K,\, t \in T \tag{7}$$

$$\sum_{(j,i)\in L^k} x_{jit}^k + s_{it}^k = b_i^k, \quad \forall\, i \in N_d^k,\, k \in K,\, t \in T \tag{8}$$

$$x_{ijt}^k - u_{ij}^k \le 0, \quad \forall\, (i, j) \in L^k,\, k \in K,\, t \in T \tag{9}$$

$$x_{ijt}^k - u_{ij}^k \beta_{it}^k \le 0, \quad \forall\, (i, j) \in L^k,\, i \in N^k,\, k \in K,\, t \in T \tag{10}$$

$$x_{ijt}^k - u_{ij}^k \beta_{jt}^k \le 0, \quad \forall\, (i, j) \in L^k,\, j \in N^k,\, k \in K,\, t \in T \tag{11}$$

$$x_{ijt}^k - u_{ij}^k \alpha_{ijt}^k \le 0, \quad \forall\, (i, j) \in L'^k,\, k \in K,\, t \in T \tag{12}$$

$$\beta_{\bar{i}t}^{\bar{k}} - \beta_{it}^k \le 0, \quad \forall\, ((i, k), (\bar{i}, \bar{k})) \in \Psi,\, t \in T \tag{13}$$

$$y_{ij}^k = \sum_{r\in R^k}\sum_{t\in T} \delta_{ijt}^{kr}, \quad \forall\, (i, j) \in L'^k,\, k \in K \tag{14}$$

$$z_i^k = \sum_{r\in R^k}\sum_{t\in T} \gamma_{it}^{kr}, \quad \forall\, i \in N'^k,\, k \in K \quad \forall\, i \in N'^k,\, k \in K \tag{15}$$

$$\alpha_{ijt}^k \le \sum_{r\in R^k}\sum_{l=1}^{t} \delta_{ijl}^{kr}, \quad \forall\, (i, j) \in L'^k,\, k \in K,\, t \in T \tag{16}$$

$$\beta_{it}^k \le \sum_{r\in R^k}\sum_{l=1}^{t} \gamma_{il}^{kr}, \quad \forall\, i \in N'^k,\, k \in K,\, t \in T \tag{17}$$

$$\sum_{(i,j)\in L'^k} \sum_{l=t}^{\min\left(\tau, t+dl_{ij}^k-1\right)} \delta_{ijl}^{kr}, \quad \forall\, k \in K,\, r \in R^k,\, t \in T \tag{18}$$

$$+ \sum_{i\in N'^k} \sum_{l=t}^{\min(\tau, t+dn_i^k-1)} \gamma_{il}^{kr} \le 1,$$

$$\sum_{t=1}^{dl_{ij}^k-1} \alpha_{ijt}^k = 0, \quad \forall\, (i, j) \in L'^k,\, k \in K \tag{19}$$

$$\sum_{t=1}^{dn_i^k-1} \beta_{it}^k = 0 \quad \forall\, i \in N'^k,\ k \in K \tag{20}$$

$$\sum_{r\in R^k}\sum_{t=1}^{dl_{ij}^k-1} \delta_{ijt}^{kr} = 0, \quad \forall\, (i, j) \in L'^k,\, k \in K \tag{21}$$

$$\sum_{r\in R^k}\sum_{t=1}^{dn_i^k-1} \gamma_{it}^{kr} = 0, \quad \forall\, i \in N'^k,\, k \in K \tag{22}$$

$$s_{it}^k \ge 0, \quad \forall\, i \in N_d^k,\, k \in K,\, t \in T \tag{23}$$

$$x_{ijt}^k \ge 0, \quad \forall\, (i, j) \in L^k,\, k \in K,\, t \in T \tag{24}$$

$$y_{ij}^k \in \{0,1\}, \quad \forall\, (i, j) \in L'^k,\, k \in K \tag{25}$$

$$z_i^k \in \{0,1\}, \quad \forall\, i \in N'^k,\, k \in K \tag{26}$$

$$\alpha_{ijt}^k \in \{0,1\}, \quad \forall\, (i, j) \in L'^k,\, k \in K,\, t \in T \tag{27}$$

$$\beta_{it}^k \in \{0,1\}, \quad \forall\, i \in N^k,\, k \in K,\, t \in T \tag{28}$$

$$\delta_{ijt}^{kr} \in \{0,1\}, \quad \forall\, (i, j) \in L'^k,\, k \in K,\, t \in T,\, r \in R^k \tag{29}$$

$$\gamma_{it}^{kr} \in \{0,1\}, \quad \forall\, i \in N'^k,\, k \in K,\, t \in T,\, r \in R^k \tag{30}$$

The first set of constraints, Eqs. (6)–(8), govern the flow conservation of node $i \in N^k$. Constraints (9)–(12) control the capacity of disrupted and undisrupted components, where Eq. (9) considers undisrupted links, Eqs. (10) and (11) consider the disrupted nodes, and Eq. (12) considers disrupted links. Constraint (13) governs the physical interdependency between nodes to ensure that node $\bar{i} \in N^{\bar{k}}$ in network

$\bar{k} \in K$ is operational at time $t \in T$ only if the node $i \in N^k$ in network $k \in K$ is also operational at time $t \in T$. Constraints (14)–(22) represent the assignment scheduling for the restoration process of disrupted components, where Eqs. (14) and (15) ensure the work crew assignment for the disrupted components if their restoration is a must, Eqs. (16) and (17)ensure the operability of a component when its restoration is completed by the specifically assigned work crew $r \in R^k$, Eq. (18) ensures that a single work crew can restore at most one disrupted component (either a link or a node) in network $k \in K$ at a specific time $t \in T$, and Eqs. (19)-(22) ensure that for a disrupted component to be functional, its restoration should be completed by the assigned work crew. Finally, constraints (23)–(30) indicate the nature of decision variables in the optimization model.

## 4. Illustrative example: interdependent networks in Shelby County, Tennessee

We apply the proposed community resilience-driven interdependent infrastructure network restoration model with data describing interdependent networks in Shelby County, Tennessee, whose location in the New Madrid Seismic Zone makes it susceptible to earthquake risk [66]. We consider three interdependent infrastructure networks: water, natural gas, and electric power distribution systems. Fig. 3 depicts the geographical layout of the infrastructure networks independently and with the consideration of their physical interdependency. The interdependent infrastructure networks consist of a total of 125 nodes including 15 demand nodes in the water network, 13 demand nodes in the gas network, and 9 demand nodes in the power network. There are total of 176 bi-directional links from all three infrastructure networks.

### *4.1. Social vulnerability in Shelby County, TN*

The SoVI-Lite algorithm [77,78] is adapted to calculate the social vulnerability indices of the demand nodes from the critical infrastructure networks in Shelby County, TN. Most of the 11 factor groups in Table 1 are addressed by the available 14 socio-economic variables listed in Table 2.

**Table 2**
District-level social vulnerability variables available in Shelby County, TN data for the SoVI-Lite algorithm.

| |
|---|
| Percentage of households earning under $75,000 annually |
| Percentage of population under the age of 5 |
| Percentage of households living below the poverty line |
| Percentage of households requiring food stamps |
| Percentage of population over the age of 65 |
| Percentage of population that is Hispanic |
| Percentage of population that is African-American |
| Percentage of population that is Asian |
| Percentage of single-female households |
| Percentage of population without a high school education |
| Percentage of population working in low-skilled service jobs |
| Percentage of population that is unemployed |
| Percentage of population speaking English as a second language |
| Percentage of population that is female |

An initial study by Barker et al. [80] explored the 14 variables for five different geographical districts in Shelby County. Fig. 4 illustrates the correlation among these 14 variables that are listed in Table 2, calculated using the Pearson correlation coefficient. Fig. 4 suggests that among these 14 variables, the intersection of with a high positive correlation (Pearson correlation coefficient $r \geq 0.85$) is visualized with dark blue. As the positive correlation decreases, the dark blue color becomes lighter. For example, the variable “75000” which stands for the percentage of household that earns less than $75,000 annually has a high positive correlation ($r \geq 0.85$) with the variable “African-American,” “Single Female,” “No Diploma,” “Food Stamp,” “Poverty,” and “Unemployed,” where these variables stand for the percentage of the population that is African-American, the percentage of single-female households, the percentage of the population that did not graduate from high school, the percentage of the households that requires social security relief such as food stamps, the percentage of the households that lives under the poverty line, and the percentage of the population that is unemployed, respectively. On the contrary, the intersection of

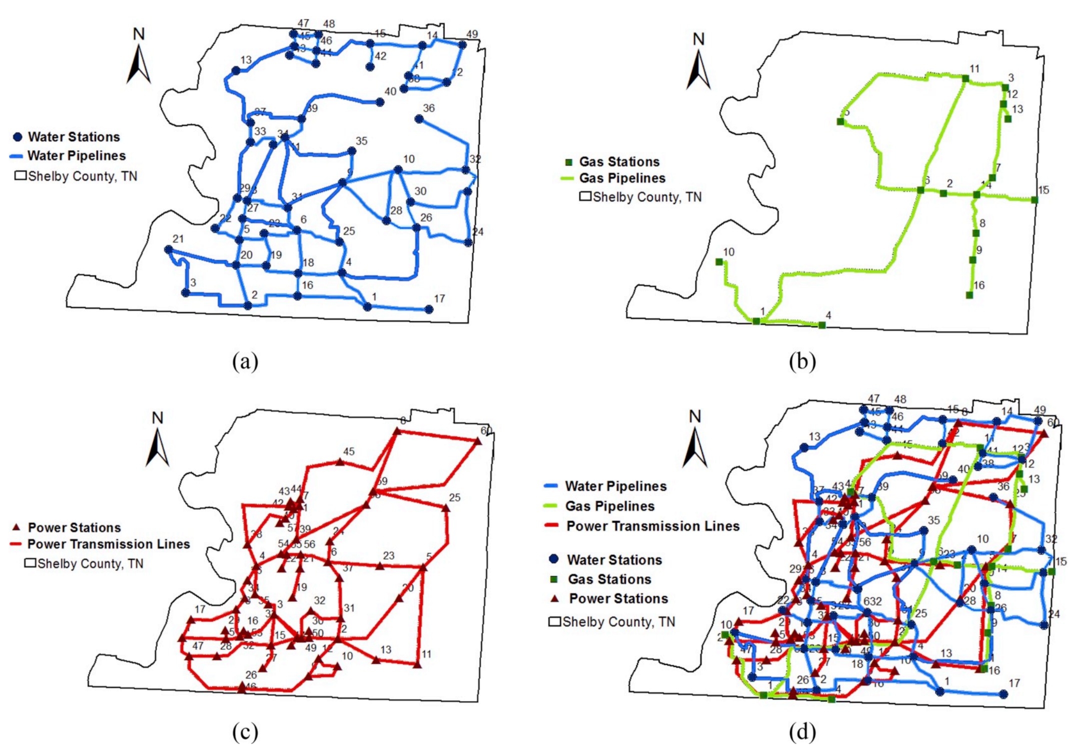


**Fig. 3.** Critical (a) water, (b) gas, and (c) power infrastructure networks of Shelby County, TN and (d) their physical interdependencies respectively (adapted from González et al. [66]).

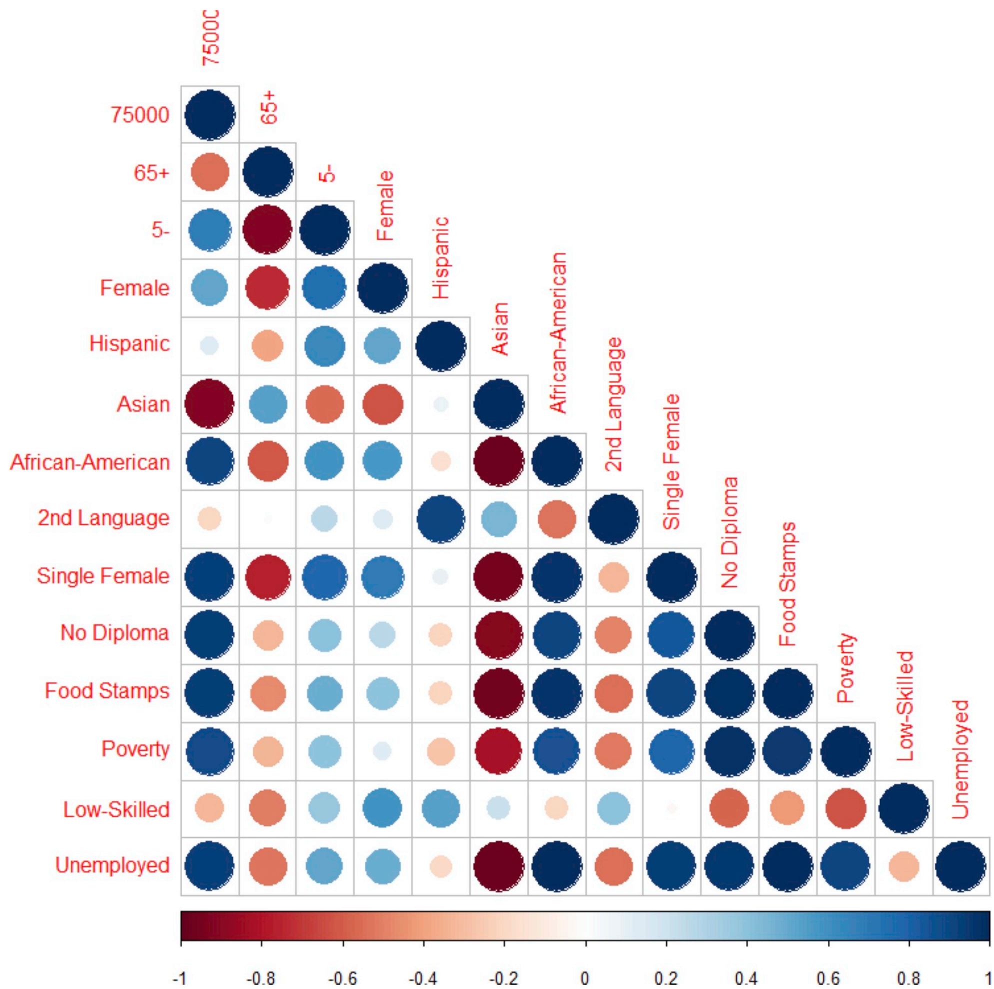


**Fig. 4.** An illustration of the correlation analysis between the 14 social vulnerability variables available for the district level in Shelby County, TN, where darker red color and bigger circle size represent a higher negative correlation and darker blue color and bigger circle size represent a higher positive correlation.

the variables that have a high negative correlation, where the Pearson correlation coefficient is below a certain value ($r \leq -0.85$), is shaded with dark red and as the negative correlation decreases, the dark red color becomes lighter. As an example, the variable "Asian," which represents the percentage of population that is Asian, has a high negative correlation ($r \leq -0.85$) with the previously explained variables "African-American," "Single Female," "No Diploma," "Food Stamp," "Poverty," and "Unemployed."

To provide a higher level of granularity for social vulnerability in Shelby County, SoVI-Lite indices are calculated at the block group level rather than the district level. A block group is a statistical division of census tracts that consists of clusters of blocks and generally contain between 600 and 3000 people who are the residents of the covered contiguous area [81]. There are 621 block groups making up Shelby County, which consists of a total of 928,794 residents. These numbers are the exact values that are utilized through the social vulnerability calculations with respect to the availability of data where around 10 block groups totaling around 4000 citizens were eliminated because certain required demographics were missing. However, not all 14 variables are available at the block group level either. Fig. 5 highlights the correlation among the eight variables available in the block group level of Shelby County, and it appears that all of the existing variables have a lower positive and negative correlation between each other when compared with the district level data. However, in the block group level data, none of the two-variable combinations have a high correlation (neither positive nor negative) behavior especially when the correlation measures in the district level are considered. In the block group level, the highest positive correlation is between the variable "75000," and the variables "African-American," "Single Female," and "Poverty," but the Pearson correlation coefficient has a lower value ($r \leq 0.6$). The definition of these variables is exactly the same with the district level variables. On the other hand, in the block group level data, none of the variable pairs end up with a Pearson correlation coefficient value that is below a certain value ($r \leq -0.6$), thus there does not exist any high negative correlation among these variables either. Further, we believe that including the social vulnerability variables that are only available at the county-level through the block group-level would bias the analysis. For example, the social vulnerability variable "2nd Language" states the percentage of population who speaks English as a second language and this data is not available in the block group-level for Shelby County, TN. However, it is available in the county-level, i.e. it is around 0.1%, which means that the percentage of the total county population that speaks English as a second language is known but it is not known for each block group separately. Therefore, summing up this county-level based single value of this particular social vulnerability variable, around 0.1%, with the other available social vulnerability variable values would harm the sensitivity of the analysis. If this step is repeated for all six social vulnerability variables that have missing data in block group-level, certain social subgroups would be counted multiple times in each block group due to the existence of high positive correlation between some of the variables, i.e. "No Diploma", "Unemployment", "Food Stamps" and etc. Hence, these recounted social subgroups could become the decision driving characteristics in the prioritization of the regions and the disrupted components that are

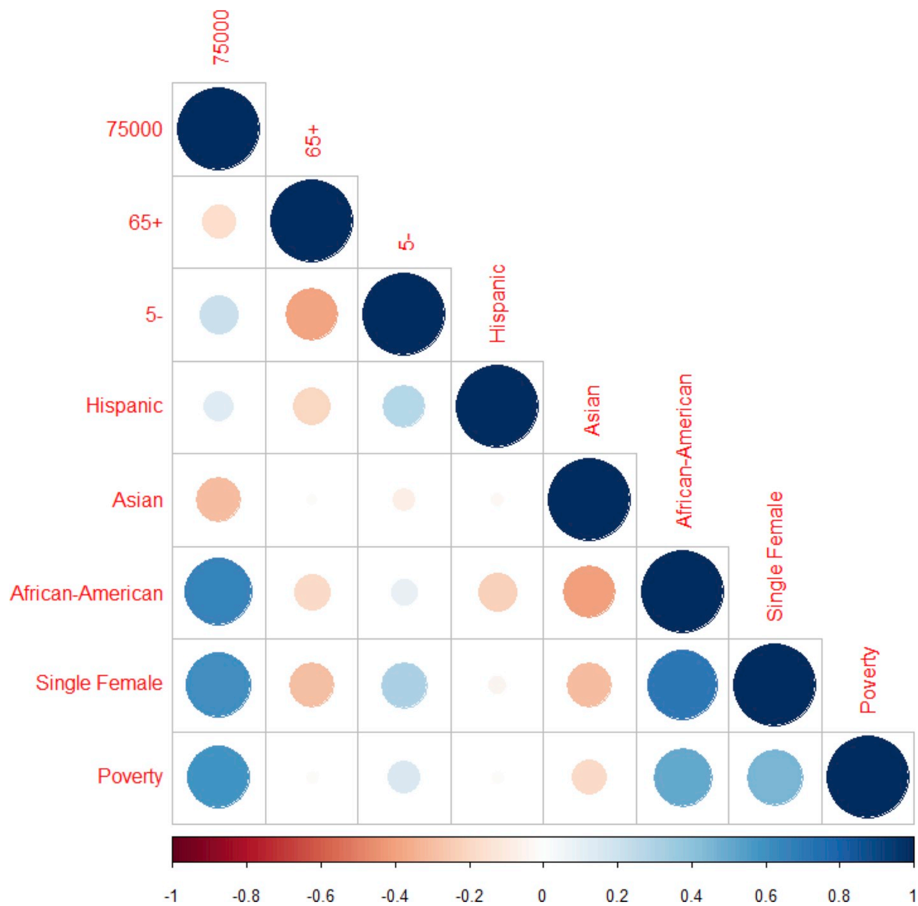


**Fig. 5.** An illustration of the correlation analysis with the available social vulnerability variables in the block group level in Shelby County, TN, where darker red color and bigger circle size represent a higher negative correlation and darker blue color and bigger circle size represent a higher positive correlation.

serving to them. But most importantly, this idea of assigning the same social vulnerability variable value for to all block groups and repeating this step for six different social vulnerability variables would conflict with the main concern of our proposed study. The mindset behind the calculation of social vulnerability scores for block groups is that "each region should be assigned with distinct social vulnerability scores due to the existence and distribution of various socioeconomic characteristics of their residents".

As such, for the block group data, all the existing variables are included in the social vulnerability calculations. Additionally, as some variables that exist in the district level data but not in the block group level data are also covered by the above analysis. For example, at the district level data, the variable "75000" and "African-American" have a highly positive correlation with the variables "No Diploma," "Food Stamp," and "Unemployment." As such, the existence of these two variables in the block group data provides insight into the three missing variables and complements the information provided with only two variables. Thus, to not lose any information, the set of all eight variables are considered in this study, as enumerated in Table 3. The SoVI-Lite calculations are based on these eight variables which contain neither high positive nor high negative correlation. Further, the correlation between the eight social vulnerability variables and the population densities of the block groups suggested neither a high positive (i.e., $r \leq 0.6$) nor a high negative (i.e., $r \leq -0.6$) correlation, suggesting that redundancy in the social vulnerability and population densities is avoided.

To assign social vulnerability scores, $V_i^k$, and population densities, $P_i^k$, to demand nodes at the block level, specific geographical regions were identified to represent each demand node. To estimate the geographical region that each demand node covers, we utilize Voronoi diagrams [82]. In essence, the Voronoi diagram method can be summarized as follows: for a given finite set of points $\{p_1, ..., p_n\}$ in the Euclidean plane, $X$, the Voronoi cell $Vor_k$ contains the point $p_k$ and all the other points whose distance to $p_k$, $d(p_x, p_k)$, is less than their distance to any other point, $p_j$, $d(p_x, p_j)$. The more formal and general definition is formulated in Eq. (31).

$$Vor_i = \{p | d(p, p_i) \leq d(p, p_j)\}, \quad \forall j \neq i, j = 1, ..., n \tag{31}$$

In this study, each demand node from all three infrastructure networks in Shelby County is considered as the Voronoi seeds and the coverage areas of the demand nodes are represented by the Voronoi cells in which they are located. These Voronoi cells, along with their associated block groups, are represented in Fig. 6. The social vulnerability indices of all the block groups that are either fully or partially included in the single Voronoi cell are assigned to the demand node that is considered as the seed of the region. The population densities are however assigned proportionally to the demand nodes according their portion that is included in each Voronoi region (i.e., for a block group

**Table 3**
The social vulnerability variables that are utilized through the SoVI-Lite algorithm for the block group level in Shelby County, TN.

| |
|---|
| Percentage of households earning under $75,000 annually |
| Percentage of population over the age of 65 |
| Percentage of population that is Asian |
| Percentage of population under the age of 5 |
| Percentage of population that is Hispanic |
| Percentage of population that is African-American |
| Percentage of single-female based households |
| Percentage of households that are in poverty |

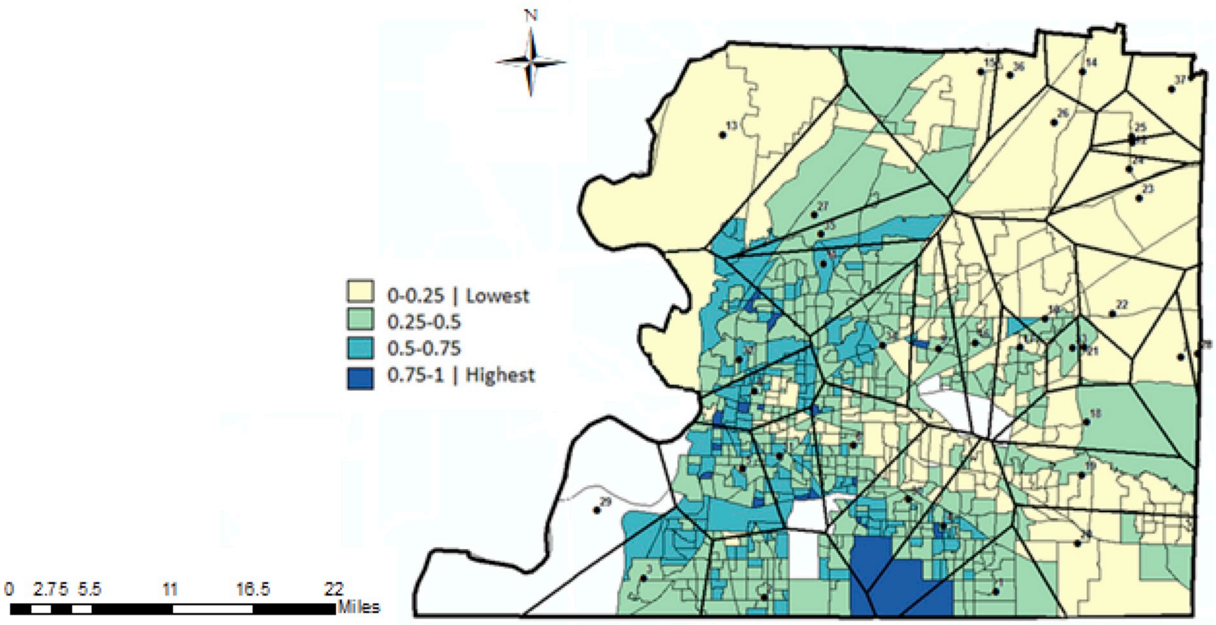


**Fig. 6.** An illustration of the distribution of block groups into Voronoi cells that are created by the demand nodes of three critical infrastructure networks in Shelby County, TN.

that is divided into two by the border of two neighbor cells, its social vulnerability index is assigned to both demand nodes, but its population is divided into two and assigned proportionally to each demand node separately). Therefore, neither the population density nor the social vulnerability score of the served area assigned to a demand node overshadows the other or solely behaves as the decision-driving parameter, but the integration of both with the amount of unmet demand at the demand node determines the order of recovery activities. Hence, even though the overall population densities of the block groups does not represent extreme differences and are considered to be relatively similar, the final weighting of the demand nodes in the mathematical model generates adequate differences in terms of importance.

The social vulnerability indices of the demand nodes are calculated by taking the average of the social vulnerability indices of the included block groups in the same Voronoi cell. Fig. 7 represents the social vulnerability indices, $SoVI_i^k$, of all the demand nodes in critical infrastructure networks of Shelby County. Fig. 8 illustrates the exponential representation of the social vulnerability scores, $V_i^k$, that are included in the optimization model to give relatively higher importance to the demand nodes in more vulnerable areas. For example, according to these figures, demand nodes 32, 5, 8, 3, and 11 represent areas that may

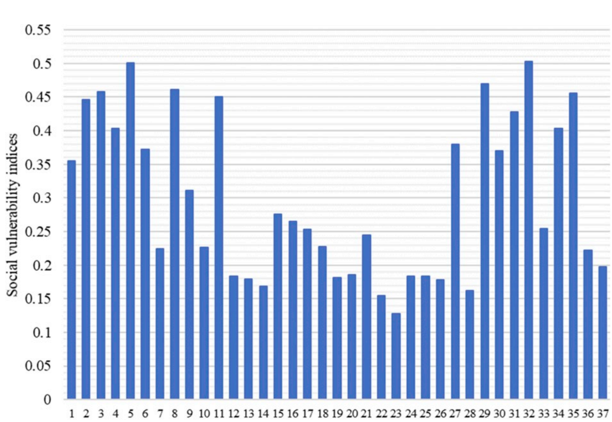


**Fig. 7.** Illustration of social vulnerability indices, $\boldsymbol{SoVI_i^k}$, of the demand nodes.

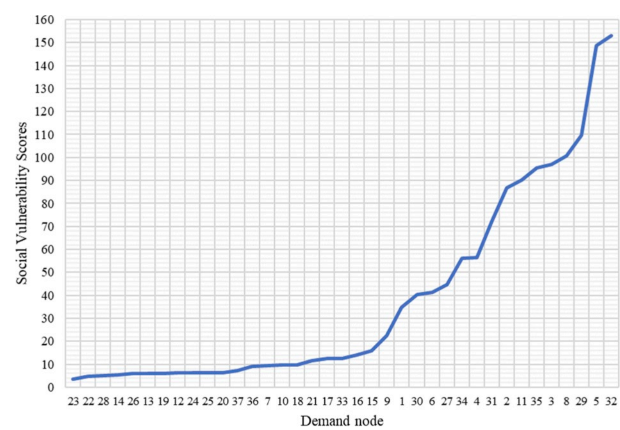


**Fig. 8.** Illustration of the exponential social vulnerability scores, $\boldsymbol{V_i^k}$.

require prior and more resources to ensure their timely restoration. Additionally, Fig. 9 represents the exponential social vulnerability scores, $V_i^k$, of the demand nodes in Shelby County to illustrate which demand nodes serve socially more vulnerable areas. The block groups that are colored white represent a lack of household information or a lack of residents.

The multi-objective problem is solved using the $\varepsilon$-constraint approach [83], where the resilience objective is converted to a constraint and assigned with the values between 0 and 1 such as $\varepsilon \in [0,1]$ as in Eq. (32). To solve the multi-objective problem, the total cost of the restoration activities is not converted into a budget constraint to support the humanitarian motivation for the work by allowing the system to recover fully.

$$\sum_{k\in K} \mu^k \sum_{t=1}^{\tau} \left( \frac{\sum_{i\in N_d^k} (Q_i^k V_i^k P_i^k) - \sum_{i\in N_d^k} (s_{it}^k V_i^k P_i^k)}{\sum_{i\in N_d^k} (\tau Q_i^k V_i^k P_i^k)} \right) \le \varepsilon \tag{32}$$

Therefore, with the introduction of the $\varepsilon$-constraint formulation for resilience, our proposed approach aims to schedule the restoration process of the interdependent infrastructure networks with the minimum total cost of restoration and disruption such that the overall

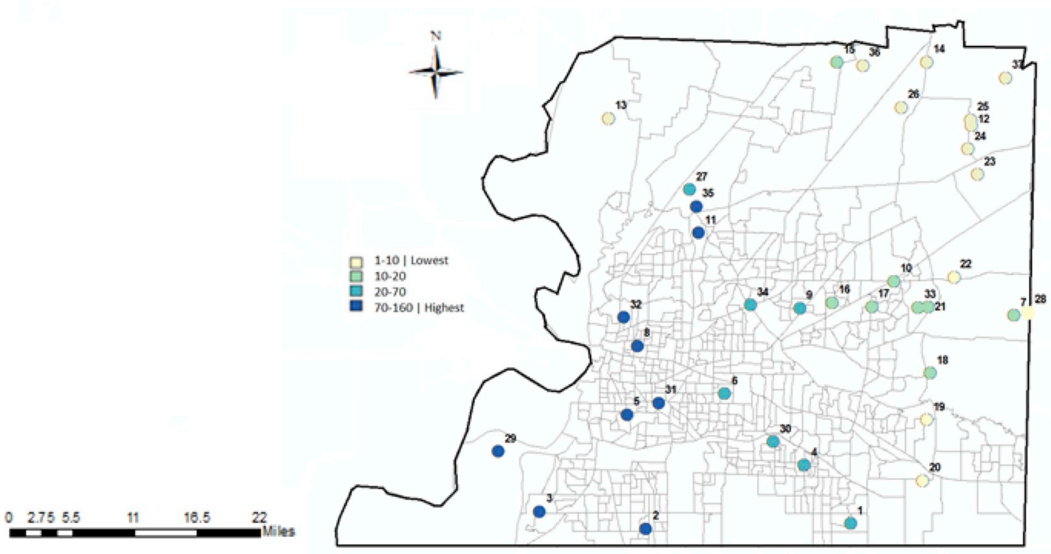


**Fig. 9.** Representation of the exponential social vulnerability scores, $V_i^k$, of the demand nodes of all three critical infrastructure networks over Shelby County, TN.

system performance would achieve the pre-determined level at the end of the recovery horizon. Through the restoration scheduling, the social vulnerability scores and the population densities of the served communities shapes the order since not prioritizing the more vulnerable and denser areas would be penalized more heavily in the system.

### 4.2. Disruption and restoration

We implement disruption scenarios each representing a different earthquake magnitude where the data is obtained from a previous study by González et al. [66]. These hypothetical earthquake scenarios ($M_w = 6$, $M_w = 7$, $M_w = 8$, $M_w = 9$) are classified as "low," "moderate," "severe," and "extremely severe," respectively, based on their increasing moment magnitude and proportional damage. The extremely severe earthquake scenario, ($M_w = 9$), results in a total of 43 disrupted components, 19 of which are demand nodes. For the restoration process, two work crews are assigned to each infrastructure network. A time horizon of 28 periods is considered to complete the recovery for all four earthquake scenarios.

Among the four disruption scenarios, the severe and extremely severe scenarios, ($M_w = 8$, $M_w = 9$), represent significant differences in the optimal restoration schedules between the inclusion and exclusion of social vulnerability and population density measures. The low and moderate earthquake scenarios, ($M_w = 6$, $M_w = 7$), contain few disrupted components and a low amount of unmet demand, therefore the inclusion of social and population measures does not result in a significant difference in restoration scheduling.

As such, we focus our analysis on the severe and extremely severe disruption scenarios, and we represent the effect of including social vulnerability and population density measures by the change in the restoration order of disrupted nodes. Fig. 10 through Fig. 12 illustrate the change in order for severe scenarios for water, gas, and power networks, respectively, and likewise Fig. 13 through Fig. 15 for extremely severe scenarios. The change in the importance of components is measured as follows: (i) the optimal restoration schedules are obtained for two separate cases: including and excluding social vulnerability and population, (ii) the restoration order of the disrupted components is listed for each network, and (iii) the difference in orders for each component is calculated with and without social vulnerability and population measures. If this difference is zero, then the restoration order of this component is the same in both cases, suggesting the importance of this component did not change between the two approaches. However, a positive difference suggests that the restoration of the component is scheduled earlier when social vulnerability and population density of its service area is taken into account, suggesting that such measures make the component a priority. Lighter shades represent components with less importance when the social vulnerability and population measures are considered. Note that the darkest shaded components might not necessarily be the most important component in the restoration scheduling, but it is the component that has the biggest change in its restoration order, thus the biggest change in its importance when additional measures are included in the optimization model. While only demand nodes are considered for weighting with social and population measures, naturally supply and transshipment nodes are important to meeting demand (at those weighted demand nodes).

The trajectory of the system performance over time under two different hypothetical earthquake magnitudes is illustrated by the change in unmet demand in Fig. 16 and Fig. 17 to compare the effect on restoration when social vulnerability and population density are accounted for in the analysis. As it can be seen from these three plots, the unmet demand over time varies for each network when community resilience measures are taken into account. According to the following illustrations, we observe that the amount of unmet demand in each network at given time $t \in T$ is more when social vulnerabilities and population densities are included in the restoration schedule. As it is formulated primarily from the community resilience perspective rather than solely the network performance perspective, our proposed approach aims to minimize the amount of unmet demand at the demand nodes that have the highest combination of social vulnerability score, population density, and unmet demand amount. That is, instead of ordering the restoration schedule based on a descending order of the amount of unmet demand, it orders the schedule based on a descending order of the social vulnerability score times population density times amount of unmet demand, $s_{it}^k \times V_i^k \times P_i^k$. Therefore, the unmet demand at the demand nodes that serve areas with higher social vulnerability, population density, and unmet demand are minimized first and then the model moves to the next disrupted component. However, at the end of the limited recovery period, both of the models, with and without considering SoVI, would accomplish leaving no unmet demand in the system.

Finally, to validate the differences between the optimal restoration schedules (without SoVI, with SoVI) for the critical infrastructure networks in Shelby County, and to highlight the contribution of the proposed study, we formulated a model to minimize the sum of differences in the restoration times of each disrupted component between the

| Disrupted water network nodes | Change in importance |
| --- | --- |
| 27 | |
| 15 | |
| 46 | |
| 42 | |
| 33 | |
| 29 | |
| 36 | |
| 21 | |
| 11 | |
| 45 | |

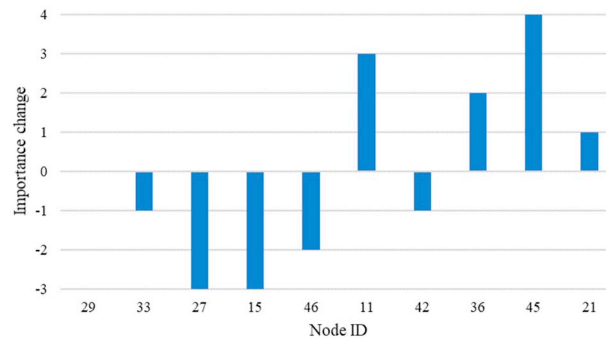


**Fig. 10.** The change in the importance of the disrupted supply, transshipment, and demand nodes in the water network when the community perspective is considered with the severe earthquake where lighter blue represents higher negative change and darker blue represents higher positive change.

| Disrupted gas network nodes | Change in importance |
| --- | --- |
| 9 | |
| 8 | |

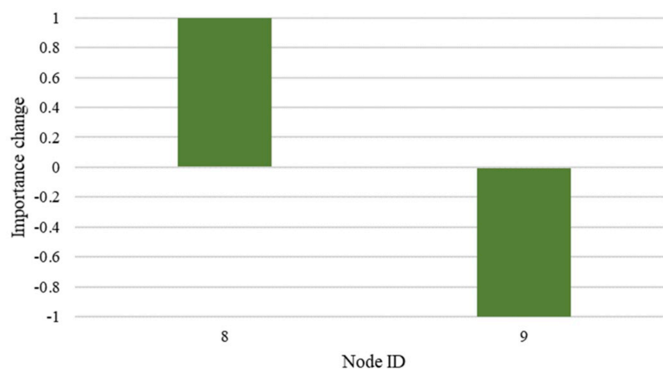


**Fig. 11.** The change in the importance of the disrupted supply, transshipment, and demand nodes in the gas network when the community perspective is considered with the severe earthquake where lighter green represents higher negative change and darker green represents higher positive change.

| Disrupted power network nodes | Change in importance |
| --- | --- |
| 33 | |
| 48 | |
| 53 | |
| 49 | |
| 24 | |
| 44 | |
| 13 | |
| 56 | |
| 21 | |
| 57 | |
| 51 | |
| 20 | |
| 1 | |

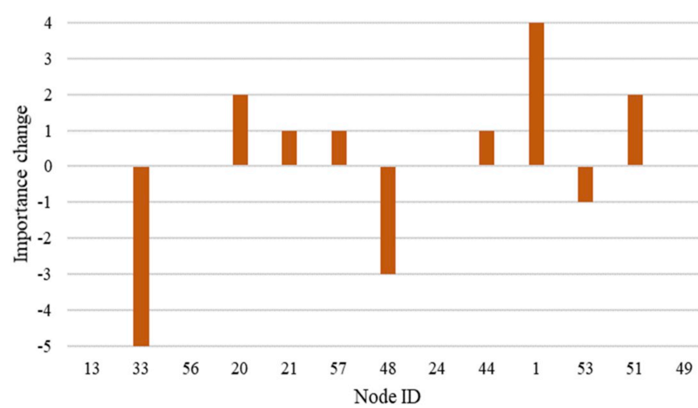


**Fig. 12.** The change in the importance of the disrupted supply, transshipment, and demand nodes in the power network when the community perspective is considered with the severe earthquake where lighter orange represents higher negative change and darker orange represents higher positive change.

without SoVI and with SoVI models. At the end, we did not find a zero distance result, suggesting that there is not one restoration schedule that is optimal for both models. Additionally, we observed that there is no restoration schedule such that the restoration of a single disrupted component is scheduled in the same order among the complete restoration schedule for both "with SoVI" and "without SoVI." For every possible alternate restoration schedule, the restoration order of a certain disrupted component is different in between the two schedules. Hence, we conclude that the speed for recovery does not overcome the social vulnerability scores of the served community. We can conclude that accounting for social vulnerability in restoration schedule indeed changes the optimal scheduling and assignment solution for the restoration of interdependent infrastructure networks after a disruptive event.

## 5. Concluding remarks

Due to the globalization of networks and the developments in the infrastructure technology, interdependencies among critical infrastructure networks are being formed incrementally. Such enhanced interdependencies result in more complex and vulnerable systems, where it becomes more challenging for the decision makers to plan their recovery after a disruptive event. Additionally, the dependency of the surrounding communities over these networks and their social vulnerabilities increase the possible impacts of the disruptive events, by hardening the problem of recovery planning both for the system and the society.

In this paper, we study the interdependent infrastructure network restoration problem and propose an optimization model from the

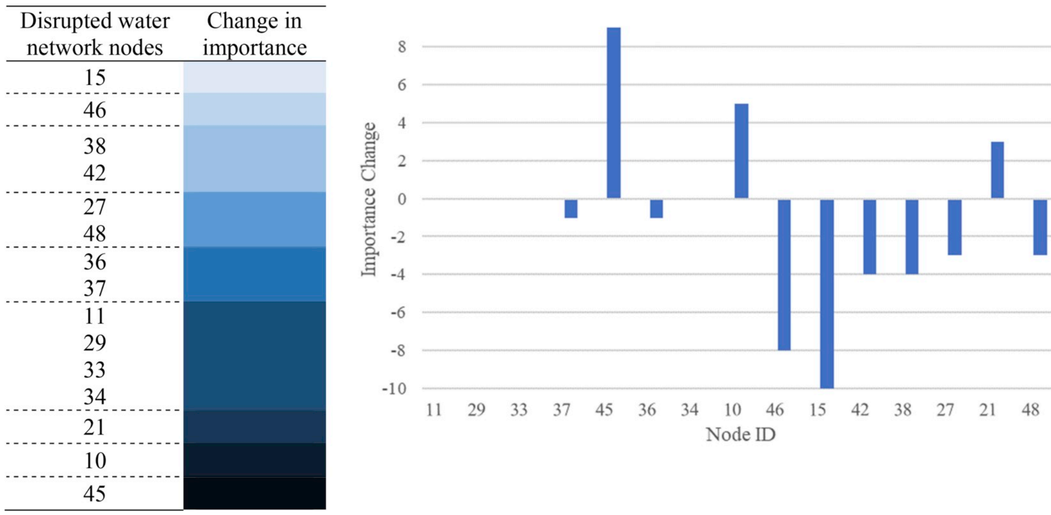


**Fig. 13.** The change in the importance of the disrupted supply, transshipment, and demand nodes in the water network when the community perspective is considered with the extremely severe earthquake where lighter blue represents higher negative change and darker blue represents higher positive change.

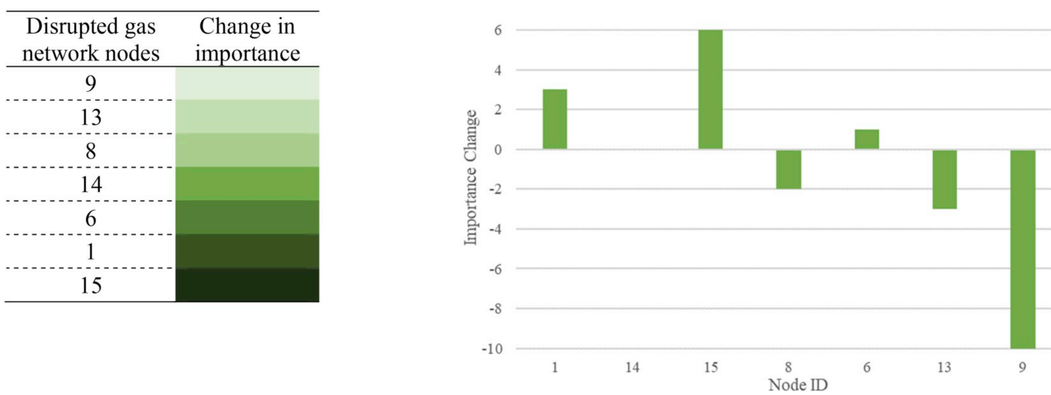


**Fig. 14.** The change in the importance of the disrupted supply, transshipment, and demand nodes in the gas network when the community perspective is considered with the extremely severe earthquake where lighter green represents higher negative change and darker green represents higher positive change.

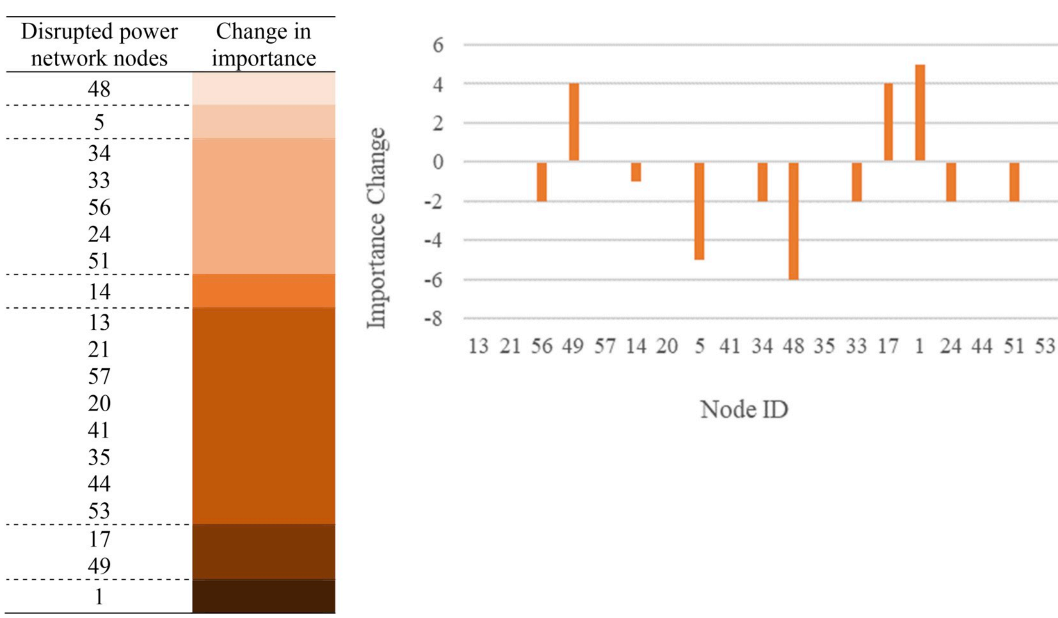


**Fig. 15.** The change in the importance of the disrupted supply, transshipment, and demand nodes in the power network when the community perspective is considered with the extremely severe earthquake where lighter orange represents higher negative change and darker orange represents higher positive change.

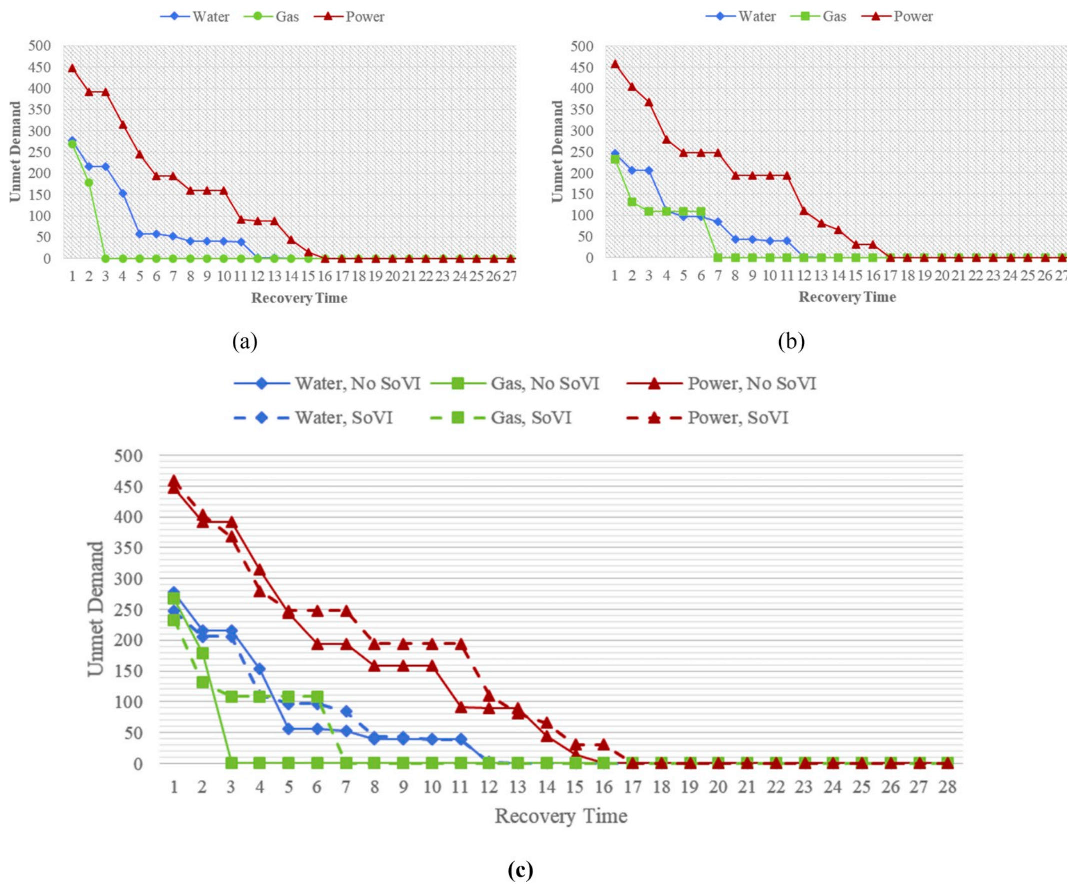


**Fig. 16.** Illustration of unmet demand over the recovery time (a) without SoVI, (b) with SoVI, and (c) comparison on the same plot where dashed lines represent the consideration and solid lines represent the inconsideration of social vulnerability and population density under a severe earthquake.

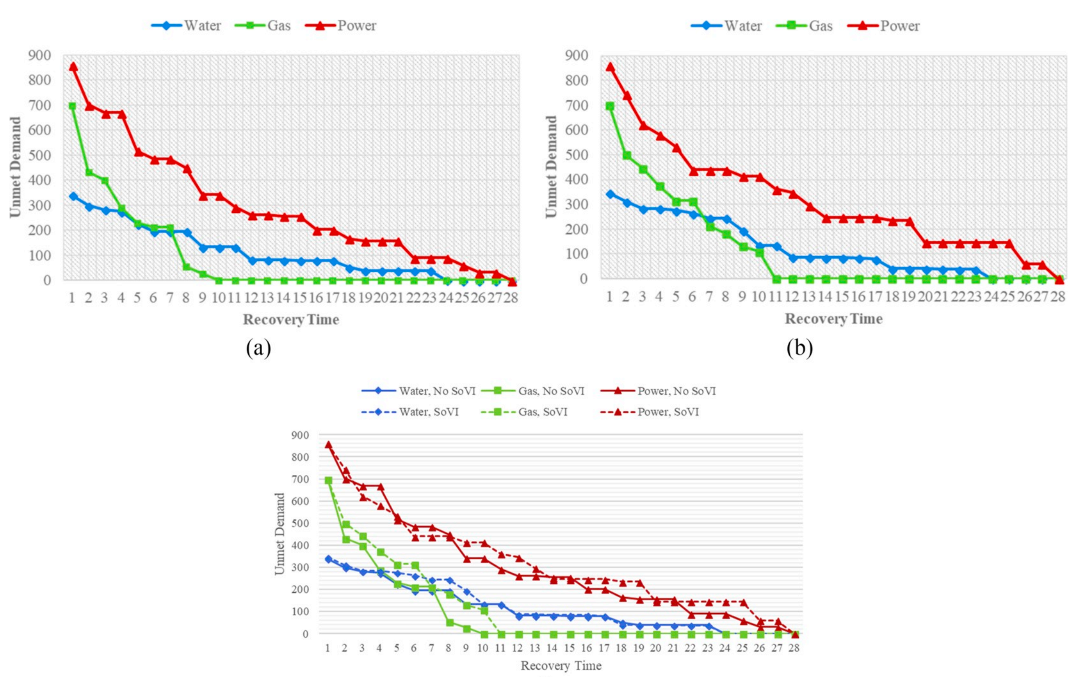


**Fig. 17.** Illustration of unmet demand over the recovery time (a) without SoVI, (b) with SoVI, and (c) comparison on the same plot where dashed lines represent the consideration and solid lines represent the inconsideration of social vulnerability and population density under an extremely severe earthquake.

community resilience perspective. Our proposed model plans the restoration schedule for each network by (i) prioritizing the disrupted components, and (ii) assigning them to available work crews for specific time periods according to their relative importance on the overall system resilience. The aim of prioritizing the disrupted components and enhancing the resilience of physically interdependent infrastructure networks consider the community resilience perspective through the restoration scheduling process as each demand node is assigned with the (i) social vulnerability score and the (ii) population density of the residential area they represent.

The social vulnerability scores are calculated with a reduced approach of Social Vulnerability Index [49], in order to account for the major social dimensions in the community, -such as age, income level, and race attainments. Also, population densities are calculated to measure the human occupancy in the surrounding of the network components. These community resilience measures are added to a mixed-integer multi-objective resilience-driven restoration model, which maximizes the cumulative community resilience of the interdependent infrastructure networks over time while considering the total cost associated with the restoration process.

As for the results of our case study, we observe that accounting for the community resilience measures in the restoration planning of interdependent infrastructure networks affects the scheduling of the disrupted components since there exists no such restoration schedule that is optimal for both including and excluding community resilience measures. As expected, disrupted components that represent socially more vulnerable and denser regions are prioritized in the restoration process. Thus, the components with higher priority correspond to not only the ones with large unmet demands in their service area, but also to the ones that are responsible for the supply and transshipment of commodities to socially more vulnerable communities.

For future work, from the network properties perspectives, the model could be extended to consider partial disruptions, such that the system can operate with reduced capacities. Moreover, partial physical dependencies could be included in the proposed model, where a component could be partially functional, if the components upon which it depends are partially operational. Other interdependent infrastructure networks that are important for completing and coordinating the recovery activities (e.g., transportation, communication) could be included. While most of the model parameters are taken from a previous study [66], the uncertainties in the system (e.g., restoration costs, restoration durations disruption scenarios) could be considered in the optimization model. From the community resilience perspective, the impacts of prioritizing the socially more vulnerable subgroups and the social implications of this strategy could be analyzed in terms of measuring the community adaptation and past disaster experience to measure the behavioral expectations and humanitarian response against disruptions better and more accurately. The dynamic nature of socioeconomic characteristics and the population densities, along with the uncertainties related to their varying existing levels, could also be included in the future studies. Naturally, a centralized decision making environment is assumed here, where a lone, central decision maker is determining schedules across all networks, and future work will address a decentralized decision making process wherein network utilities make restoration decisions with their own information. Furthermore, the proposed community resilience-based prioritization and scheduling process could be combined with geographical hazard metrics to account for spatial risks associated with the specific location of the network components. Lastly, a benchmark analysis for comparing the obtained results of the proposed approach and the heuristic.

## Acknowledgment

This work was supported in part by the National Science Foundation through awards 1541165 and 1635813.

## References

[1] The Report of the President's Commission on Critical Infrastructure Protection, Critical Foundation: Protecting America's Infrastructure, USA, 1997.
[2] The Infrastructure Security Partnership, Regional Disaster Resilience Guide for Developing an Action Plan, Technical report American Society of Civil Engineers, 2011.
[3] B.H. Obama, Critical Infrastructure Security and Resilience, The White House, Washington, 2013.
[4] Department of Homeland Security, National Preparedness Report, (2013).
[5] A.L. Barabasi, R. Albert, Emergence of scaling in random networks, Science 286 (5439) (1999) 509–512.
[6] A.J. Holmgren, Using graph models to analyze the vulnerability of electric power networks, Risk Anal.: Int. J. 26 (4) (2006) 955–969.
[7] A. Nagurney, Q. Qiang, Fragile Networks: Identifying Vulnerabilities and Synergies in an Uncertain World, John Wiley & Sons, 2009.
[8] M.E.J. Newman, P. Holme, E.A. Leicht, Vertex similarity in networks, Phys. Rev. 73 (2) (2006) 026120.
[9] J. Johansson LaRocca, H. Hassel, S. Guikema, Topological performance measures as surrogates for physical flow models for risk and vulnerability analysis for electric power systems, Risk Anal.: Int. J. 35 (4) (2014) 608–623.
[10] C.D. Nicholson, K. Barker, J.E. Ramirez-Marquez, Flow-based vulnerability measures for network component importance: experimentation with preparedness planning, Reliab. Eng. Syst. Saf. 145 (2016) 62–73.
[11] M. Ouyang, Review on modeling and simulation of interdependent critical infrastructure systems, Reliab. Eng. Syst. Saf. 121 (2014) 43–60.
[12] C.M. Rocco, J.E. Ramirez-Marquez, D.E. Salazar, I. Hernandez, Implementation of multi-objective optimization for vulnerability analysis of complex networks, Proc. Inst. Mech. Eng. O J. Risk Reliab. 224 (2) (2010) 87–95.
[13] N. Xu, S.D. Guikema, R. Davidson, L. Nozick, Z. Cagnan, K. Vaziri, Optimizing scheduling of post-earthquake electric power restoration tasks, Earthq. Eng. Struct. Dyn. 36 (2) (2007) 265–284.
[14] S. Yan, Y.L. Shih, Optimal scheduling of emergency roadway repair and subsequent relief distribution, Comput. Oper. Res. 36 (6) (2009) 2049–2065.
[15] T.C. Matisziw, A.T. Murray, T.H. Grubesic, Strategic network restoration, Network. Spatial Econ. 10 (3) (2010) 345–361.
[16] S.G. Nurre, B. Cavdaroglu, J.E. Mitchell, T.C. Sharkey, Restoring infrastructure systems: an integrated network design and scheduling (INDS) problem, Eur. J. Oper. Res. 223 (3) (2012) 794–806.
[17] D.T. Aksu, L. Ozdamar, A mathematical model for post-disaster road restoration: enabling accessibility and evacuation, Transport. Res. Part E: Logistics and Transportation 61 (1) (2014) 56–67.
[18] E.D. Vugrin, M.A. Turnquist, N.J. Brown, Optimal recovery sequencing for enhanced resilience and service restoration in transportation networks, Int. J. Crit. Infrastruct. 10 (3–4) (2014) 218–246.
[19] S. Kamamura, D. Shimazaki, K. Genda, K. Sasayama, Y. Uematsu, Disaster recovery for transport network through multiple restoration stages, IEICE Trans. Commun. 98 (1) (2015) 171–179.
[20] Y.P. Fang, N. Pedroni, E. Zio, Resilience-based component importance measures for critical infrastructure network systems, IEEE Trans. Reliab. 65 (2) (2016) 502–512.
[21] S.M. Rinaldi, J.P. Peerenboom, T.K. Kelly, Identifying, understanding and analyzing critical infrastructure interdependencies, IEEE Control Syst. Mag. 21 (6) (2001) 11–25.
[22] M. Castells, The Rise of the Network Society. The Information Age: Economy, Society, and Culture Volume I (Information Age Series), (1996) (London: Blackwell).
[23] S. Graham, Constructing premium network spaces: reflections on infrastructure networks and contemporary urban development, Int. J. Urban Reg. Res. 24 (1) (2000) 183–200.
[24] S. Saidi, L. Kattan, P. Jayasinghe, P. Hettiaratchi, J. Taron, Integrated infrastructure systems: a review, Sustainable Cities and Society 36 (2018) 1–11.
[25] S.V. Buldyrev, R. Parshani, G. Paul, H.E. Stanley, S. Havlin, Catastrophic cascade of failures in interdependent networks, Nature 464 (7291) (2010) 1025–1028.
[26] I. Eusgeld, C. Nan, S. Dietz, "System-of-systems" approach for interdependent critical infrastructures, Reliab. Eng. Syst. Saf. 96 (6) (2011) 679–686.
[27] R.G. Little, Controlling cascading failure: understanding the vulnerabilities of interconnected infrastructures, J. Urban Technol. 9 (1) (2002) 109–123.
[28] W.A. Wallace, D.M. Mendonca, E.E. Lee, J.E. Mitchell, J.H. Chow Wallace, J.L. Monday, Managing disruptions to critical interdependent infrastructures in the context of the 2001 World Trade Center attack, Beyond September 11th: an Account of Post-Disaster Research, Natural Hazards Research and Applications Information Center, University of Colorado, 2003, pp. 165–198 special publication #39.
[29] R. Holden, D.V. Val, R. Burkhard, S. Nodwell, A network flow model for interdependent infrastructures at the local scale, Saf. Sci. 53 (1) (2013) 51–60.
[30] P.M. Baidya, W. Sun, Effective restoration strategies of interdependent power system and communication network, J. Eng. 1 (1) (2017).
[31] K. Barker, J.H. Lambert, C.W. Zobel, A.H. Tapia, J.E. Ramirez-Marquez, L.A. McLay, C.D. Nicholson, C. Caragea, Defining resilience analytics for interdependent cyber physical-social networks, Sustainable and Resilient Infrastructure 2 (2) (2017) 59–67.
[32] National Academies of Science, Disaster Resilience: A National Imperative, (2012).
[33] J. Rotmans, W.E. Walker, P. Harremoës, J.P. van der Sluijs, M.B.A. van Asselt, P. Janssen, M.P.K. von Krauss, Defining uncertainty: a conceptual basis for uncertainty management in model-based decision support, Integr. Assess. 4 (1) (2003) 5–17.
[34] Resilience Alliance, Adaptive Capacity, (2009).
[35] United Nations, Yokohama strategy and plan of action for a safer world: guidelines for natural disaster prevention, preparedness, and mitigation, Paper Read at World Conference on Natural Disaster Reduction, at Yokokhama, 1994.
[36] S.L. Cutter, L. Barnes, M. Berry, C. Burton, E. Evans, E. Tate, J. Webb, A place-based model for understanding community resilience to natural disasters, Glob. Environ. Chang. 18 (4) (2008) 598–606.

[37] G.A. Tobin, Sustainability and community resilience: the holy grail of hazards planning? Glob. Environ. Chang. B Environ. Hazards 1 (1) (1999) 13–25.
[38] D. Mileti, Disasters by Design: A Reassessment of Natural Hazards in the United States. Natural Hazards and Disasters: Reducing Loss and Building Sustainability in a Hazardous World: A Series, Joseph Henry Press, 1999.
[39] G.F. White, J.E. Haas, Assessment of Research on Natural Hazards, MIT Press, Cambridge, MA, 1975.
[40] G. Bonanno, Loss, trauma, and human resilience: have we underestimated the human capacity to thrive after extremely aversive events? Am. Psychol. 59 (2004) 20–28.
[41] L. L. Morland Butler, G. Leskin, Psychological resilience in the face of terrorism, in: B. Bongar, L. Brown, L. Beutler, J. Breckenridge, P. Zimbardo (Eds.), Psychology of Terrorism, 2007, pp. 400–417.
[42] D. Brown, J. Kulig, The concept of resiliency: theoretical lessons from community research, Health and Canadian Society 4 (1997) 29–52.
[43] C. Sonn, A. Fisher, Sense of community: community resilient responses to oppression and change, J. Community Psychol. 26 (1998) 457–472.
[44] W. Adger, Social and ecological resilience: are they related? Prog. Hum. Geogr. 24 (2000) 347–364.
[45] D. Godschalk, Urban hazard mitigation: creating resilient cities, Nat. Hazards Rev. 4 (2003) 136–143.
[46] Berkes, F. and H. Ross. Community resilience: toward and integrated approach, Soc. Nat. Resour., 26(1): 5-20.
[47] F.H. Norris, S.P. Stevens, B. Pfefferbaum, K.F. Wyche, R.L. Pfefferbaum, Community resilience as a metaphor, theory, set of capacities, and strategy for disaster readiness, Am. J. Community Psychol. 41 (1–2) (2007) 127–150.
[48] Subcommittee on Disaster Risk Reduction, Grand Challenges for Disaster Reduction, National Science and Technology Council, Washington, DC, 2005.
[49] S.L. Cutter, B.J. Boruff, W.L. Shirley, Social vulnerability to environmental hazards, Soc. Sci. Q. 84 (1) (2003) 242–261.
[50] Y.Y. Haimes, On the definition of resilience in systems, Risk Anal.: Int. J. 29 (4) (2009) 498–501.
[51] T. Aven, On some recent definitions and analysis frameworks for risk, vulnerability, and resilience, Risk Anal.: Int. J. 31 (4) (2010) 515–522.
[52] B.M. Ayyub, P.E.F. Asce, Vulnerability, uncertainty, and risk: analysis, modelling and management, Proceedings of the ICVRAM 2011, 2011.
[53] S. Hosseini, K. Barker, J.E. Ramirez-Marquez, A review of definitions and measures of system resilience, Reliab. Eng. Syst. Saf. 145 (2016) 47–61.
[54] G. Cimellaro, A. Reinhorn, M. Bruneau, Seismic resilience of a hospital system, Structure and Infrastructure Engineering 6 (1) (2010) 127–144.
[55] D.J. Rosenkrantz, S. Goel, S.S. Ravi, J. Gangolly, Resilience metrics for service-oriented networks: a service allocation approach, IEEE Transactions on Services Computing 2 (3) (2009) 183–196.
[56] Y. Li, B.J. Lence, Estimating resilience of water resources systems, Water Resour. Res. 43 (7) (2007) W07422.
[57] D. Henry, J.E. Ramirez-Marquez, Generic metrics and quantitative approaches for system resilience as a function of time, Reliab. Eng. Syst. Saf. 99 (1) (2012) 114–122.
[58] K. Barker, J.E. Ramirez-Marquez, C.M. Rocco, Resilience-based network component importance measures, Reliab. Eng. Syst. Saf. 117 (2013) 89–97.
[59] H. Jönsson, J. Johansson, H. Johansson, Identifying critical components in technical infrastructure networks, Journal of Risk and Reliability 222 (2) (2008) 235–243.
[60] A. Rose, Economic resilience to natural and man-made disasters: multidisciplinary origins and contextual dimensions, Environ. Hazards 7 (4) (2007) 383–398.
[61] E.E. Lee, J.E. Mitchell, W.A. Wallace, Restoration of services in interdependent infrastructure systems: a network flows approach. *Systems, Man, and Cybernetics, Part C: Applications and Reviews*, IEEE Transactions on 37 (6) (2007) 1303–1317.
[62] J. Gong, E.E. Lee, J.E. Mitchell, W.A. Wallace, Logic-based multiobjective optimization for restoration planning, Optimization and Logistics Challenges in the Enterprise, Springer US, 2009, pp. 305–324.
[63] C. Coffrin, P. Van Hentenryck, R. Bent, Last-mile restoration for multiple interdependent infrastructures, Proceedings of the 26th AAAI Conference on Artificial Intelligence, Toronto, Canada, July 22–26, vol. 12, 2012, pp. 455–463.
[64] B. Cavdaroglu, E. Hammel, J.E. Mitchell, T.C. Sharkey, W.A. Wallace, Integrating restoration and scheduling decisions for disrupted interdependent infrastructure systems, Ann. Oper. Res. 203 (1) (2013) 279–294.
[65] T.C. Sharkey, B. Cavdaroglu, H. Nguyen, J. Holman, J.E. Mitchell, W.A. Wallace, Interdependent network restoration: on the value of information-sharing, Eur. J. Oper. Res. 244 (1) (2015) 309–321.
[66] A.D. González, L. Dueñas-Osorio, M. Sánchez-Silva, A.L. Medaglia, The interdependent network design problem for optimal infrastructure system restoration, Comput. Aided Civ. Infrastruct. Eng. 31 (5) (2016) 334–350.
[67] A.M. Smith, A.D. González, L. Dueñas-Osorio, R.M. D'Souza, Interdependent Network Recovery Games, Risk Anal. (2017), https://doi.org/10.1111/risa.12923.
[68] A.D. González, A. Chapman, L. Dueñas-Osorio, M. Mesbahi, R. D'Souza, Efficient restoration strategies using the recovery operator, Comput. Aided Civ. Infrastruct. Eng. 32 (12) (2017) 991–1006.
[69] D.Z. Tootaghaj, N. Bartolini, H. Khamfroush, T. La Porta, Controlling cascading failures in interdependent networks under incomplete knowledge, Proceedings of the IEEE 36th Symposium on Reliable Distributed Systems, 2017, Hong Kong, September 26-29, 2017, pp. 54–63.
[70] C. Zhang, J.J. Kong, S.P. Simonovic, Restoration resource allocation model for enhancing resilience of interdependent infrastructure systems, Saf. Sci. 102 (2018) 169–177.
[71] Y. Almoghathawi, K. Barker, L. Albert, Resilience-driven restoration model for interdependent infrastructure networks, Reliab. Eng. Syst. Saf. 185 (2019) 12–23.
[72] National Research Council, Facing Hazards and Disasters: Understanding Human Dimensions, National Academies Press, 2006.
[73] K. Tierney, Disaster Response: Research Findings and Their Implications for Resilience Measures vol. 6, CARRI Research Report, Oak Ridge, TN, 2009.
[74] E. Auf der Heide, J. Scanlon, Health and Medical Preparedness and Response, Emergency management: Principles and practice for local government, 2007, pp. 183–206.
[75] B.H. Morrow, Identifying and mapping community vulnerability, Disasters 23 (1) (2002) 1–18.
[76] P. Blaikie, T. Cannon, I. Davis, B. Wisner, At Risk: Natural Hazards, People's Vulnerability and Disasters, (1994) (Routledge).
[77] S.L. Cutter, C.T. Emrich, D.P. Morath, C.M. Dunning, Integrating social vulnerability into federal flood risk management planning, Journal of Flood Risk Management 6 (4) (2013) 332–344.
[78] J.M. Evans, D. Hardy, M. Hauer, Assessing Social Vulnerability Using "SoVI-Lite:" A Demonstration Study at Glynn County, (2014) (GA).
[79] N. Morshedlou, A.D. González, K. Barker, Work crew routing problem for infrastructure network restoration, Transport. Res. Part B 118 (2018) 66–89.
[80] K. Barker, D.B. Karakoc, Y. Almoghathawi, Interdependent infrastructure network restoration problem from a community-resilience perspective, Proceedings of the European Safety and Reliability Conference, Trondheim, NOR, 2018.
[81] US Census Bureau, Geographic Terms and Concepts, (2010).
[82] A. Okabe, T. Satoh, T. Furuta, A. Suzuki, K. Okano, Generalized network Voronoi diagrams: concepts, computational methods, and applications, Int. J. Geogr. Inf. Sci. 22 (9) (2008) 965–994.
[83] V. Chankong, Y.Y. Haimes, Multiobjective Decision Making: Theory and Methodology, Dover Books on Engineering. Courier Dover Publications, 2008.
[84] S. Graham, Introduction: cities and infrastructure, Int. J. Urban Reg. Res. 24 (1) (2000) 114–119.
[85] T.P. McAllister, Community Resilience of the Built Environment, National Institute of Standards and Technology, 2012.